Defects in epitaxial insulating thin films

1999 J. Phys.: Condens. Matter 11 9943

(http://iopscience.iop.org/0953-8984/11/49/312)

J. Phys.: Condens. Matter **11** (1999) 9943–9954. Printed in the UK PII: S0953-8984(99)04447-1

Defects in epitaxial insulating thin films

C Tegenkamp, H Pfnür†, W Ernst, U Malaske, J Wollschläger, D Peterka, K M Schröder, V Zielasek and M Henzler

Institut für Festkörperphysik, Universität Hannover, Appelstraße 2, D-30167 Hannover, Germany

E-mail: pfnuer@fkp.uni-hannover.de (H Pfnür)

Received 18 May 1999, in final form 18 August 1999

Abstract. Defects on thin epitaxial insulator films of NaCl(100), KCl(100), and MgO(100) generated during growth and by electron bombardment are investigated by high-resolution spot profile analysis in low-energy electron diffraction (SPALEED), photoelectron spectroscopy (XPS, UPS), electron energy-loss spectroscopy (EELS), and thermal desorption spectroscopy (TDS). All three insulators contain morphological defects: NaCl overgrows the monatomic Ge(100) steps in a carpet-like mode, whereas KCl grown on NaCl(100) forms a regular array of stacking faults up to three monolayers of KCl, and the MgO film grown on Ag(100) reveals a broadened (1×1) pattern in LEED due to the formation of mosaics. In EELS, surface colour centres, produced by electron bombardment, on NaCl induce losses at 2.1 eV for F_S centres and at 1.5 eV for M_S centres and on KCl induce losses at 1.6 eV and 1.0 eV, respectively. Close to room temperature, high electron exposures result in additional losses in the band gap due to surface and bulk plasmons of Na and K clusters. A similar anion vacancy defect structure on MgO with losses at 2.1 eV and 3.3 eV can be produced by incomplete desorption of metallic Mg from the MgO(100) surface. TDS experiments show that colour centres increase the binding energy of Kr physisorbed on NaCl(100) by about 25%. The concentration of point defects was determined by titration with noble gases in thermal desorption.

1. Introduction

Alkali halides as well as MgO are prototype wide-band-gap insulators, the bulk properties of which have been studied extensively in the past [1–3]. However, investigations of insulating surfaces were limited to a small number of surface-sensitive techniques due to the charging of the bulk insulating material. This problem can mostly be circumvented by use of thin insulating films epitaxially grown on conducting substrates, which show only slight charging effects [4, 5].

Perfect defect-free insulating surfaces are highly inert [3]. However, they may become chemically reactive once defects (isolated vacancies, steps, etc) are formed. In fact, surfaces are never free of defects. Therefore, it is of considerable relevance to study the properties of various defects on such surfaces. Epitaxial insulator films are relatively easy to produce and allow, via the choice among various substrates, modifications of the kind of defect and of their concentration. Good characterization of their geometric and electronic properties is a necessary pre-condition for a controlled manipulation of the properties of such films.

In this paper we try to demonstrate the variability of defects by characterizing their geometric and electronic properties. The defects are extended ones, as obtained by epitaxial

† Author to whom any correspondence should be addressed.

0953-8984/99/499943+12$30.00

thin-film growth, due to the lateral and vertical mismatch between the adsorbed film and the substrate. In a second step we report on anion vacancies produced on these films. They act as colour centres by introducing new electronic states in the band gaps. This is the origin of the chemical reactivity of these surfaces. As will be shown in the last part, titration of these point defects with noble gases allows the determination of their concentration, and gives more insight into their thermodynamical role in the context of phase equilibria on these surfaces.

2. Experiment

The experiments for the NaCl and MgO epitaxy have been carried out in different UHV chambers at base pressures lower than 1×10^{-8} Pa. For studies of the morphology of the insulator surfaces and of the corresponding substrates, the chambers were equipped with a high-resolution spot profile analysis LEED (SPALEED) instrument. The electronic structure was studied using He I and He II radiation for UPS, and a twin anode with Mg and Al targets for XPS. For EELS we used partly conventional electron guns, and partly monochromatized electron beams with an energy width down to 5 meV. The backscattered electrons from the EELS and the photoelectrons were detected by spherical analysers. Both the Ge(100) and the Ag(100) samples used as substrates were mounted on transferable holders. The samples were heated either by a combination of radiation from a tungsten filament located behind the crystals and of electron bombardment or by direct current. The temperature was controlled by thermocouples (Ni/Ni–Cr) spot welded to the sample surface (Ag) or to the crystal mount (Ge) and a computerized temperature controller with a resolution of 0.1 K, which also allowed linear temperature ramps.

Both (100)-oriented surfaces were polished by diamond pastes down to 0.25 μm grain size in several steps, and in the case of Ag by a further chemo-mechanical treatment [6]. Both samples were cleaned by sputtering with Ar^+ ions and subsequent annealing (Ge: at 300 K for 60 min at 800 eV, annealing up to 1100 K, with a crystal current of 1.5 μA; Ag: at 350 K for 30 min at 2 keV, annealing up to 700 K, with a crystal current of 10 μA) until LEED revealed a sharp (1×1) pattern for Ag(100) at room temperature and a c(2×4) pattern for Ge(100) at temperatures lower than 200 K.

NaCl was evaporated from an Al_2O_3 tube filled with NaCl and heated by a tungsten wire onto the Ge(100) surface at temperatures around 170 K, and this was followed by subsequent annealing to 550 K. The KCl films were produced in a similar way, by evaporation of KCl onto the NaCl(100) film at temperatures of 200 K and annealing to 300 K.

For growth experiments on MgO, we evaporated metallic Mg from an Al_2O_3 crucible in an O_2 background pressure of 5×10^{-5} Pa at a substrate temperatures of 350 K, and this was followed by annealing up to 500 K.

TDS experiments were carried out in front of a QMS (Balzers) equipped with a shield around the ionizer that acted as a stagnation tube. Thus the sensitivity was increased and the background from the sample holder strongly reduced. The Kr atoms were deposited through a cooled doser onto the NaCl surface in order to minimize contamination.

3. Results and discussion

3.1. Morphology and stoichiometry: defects during growth

NaCl deposited on Ge(100) at surface temperatures below 200 K grows in a layer-by-layer mode in (1×1) periodicity, since the lattice constants of NaCl (5.65 Å) and Ge (5.66 Å) match closely. The smallest step heights, however, differ by a factor of 2 due to the different

crystal structures. In order to avoid large repulsive forces between ions of equal charge, the NaCl(100) overgrows the monatomic steps of Ge(100) as an elastic carpet. As revealed by a detailed LEED profile analysis [7], the NaCl film is elastically slightly strained and tilted across these steps, whereas far away from the steps NaCl grows in registry with the flat Ge(100) terraces. Typical lengths of the bent parts of the films are between 20 and 30 Å. This well known growth mode of NaCl does not seem to be specific to the growth on a Ge(100) surface. This carpet growth mode was also found, e.g., for NaCl/Al(111) [8] and for NaCl/Cu(211) [9].

On evaporation of KCl on NaCl(100), several stages of growth are observed [10, 11]: up to a coverage of one monolayer, additional satellite spots around the diffraction spots of the underlying NaCl(100) film are seen with LEED; their positions correspond to the lattice misfit of 10% between KCl and NaCl. This so-called floating mode [11] transforms in the coverage regime between 2 and 3 ML into a new phase with spots at 3/4 positions with respect to the NaCl(100) surface. These cannot be attributed to the lattice mismatch any longer. Instead, the KCl film forms a regular array of stacking faults along the (111) glide planes [10] in order to reduce the strain in the film. Films thicker than 4 ML grow with their own lattice constant.

MgO(100) films, generated by evaporation of various amounts of Mg onto the Ag surface at temperatures between 200 K and 300 K and oxidized afterwards by exposures to up to 50 L of oxygen, are not fully oxidized. Only in the topmost four layers can stoichiometric MgO be generated with a residual metallic Mg film between the Ag(100) substrate and the insulating film, as seen with XPS and Auger spectroscopy [12]. Annealing for several minutes at 700 K reveals a ring structure in LEED containing twelve diffuse first-order diffraction spots due to the three domains of (100)-oriented MgO crystallites rotated by 120°. The orientational order obviously remains from the hexagonally ordered Mg film [13, 14]. These incompletely oxidized films are difficult to characterize further. Therefore, we evaporated Mg in an oxygen background pressure to obtain fully oxidized Mg. For a deposition rate of 1 ML min^{-1} of Mg in an oxygen background pressure of 3×10^{-5} Pa or higher at a substrate temperature between 300 K and 500 K, the MgO films show the best quality with regard to morphology and stoichiometry. The MgO films grow layer by layer, as seen both from intensity oscillations of the (00) beam with LEED [15] and from the linear increase of the Mg 1s emission, measured with XPS, followed by the characteristic change of slope when the first monolayer is completed [16]. A typical LEED pattern of these MgO(100) films is shown in figure 1. However, line scans of the specular diffraction peak along the [001] and [010] directions show additional satellites around the (00) spot which shift with increase of the electron energy. A detailed spot profile analysis reveals that the satellites are due to the formation of mosaics tilted by 2.9° and 1.5° away from the [001] direction. As concluded from the FWHM of the diffraction spots at an out-of-phase condition, the lateral dimensions of the mosaics are between 20 and 30 lattice constants [12]. A model of the corresponding adlayer morphology is presented in the right-hand part of figure 1.

Besides containing these morphological defects as imperfections, the MgO films generated as described turn out to also be non-stoichiometric at the surface. The evaporation of metallic Mg in a molecular oxygen atmosphere results in the formation of an MgO_2 species, as seen from the double-peak structure of the O 1s emission, measured with XPS, and shown in the left-hand part of figure 2 for various amounts of MgO. The main peak located at 531 eV binding energy (the LBE peak) is accompanied by a shoulder at approximately 2.5 eV higher binding energy (the HBE peak). With increasing coverage, the double peak shifts by 0.8 eV to higher binding energies, while the peak splitting remains constant. For thicker layers no further peak shifts are found. This peak structure seems to be specific to MgO surfaces generated in the way described above, since similar results have been obtained also for MgO grown on Mo(100) [17–19]. There is now common agreement that the energetic peak position of

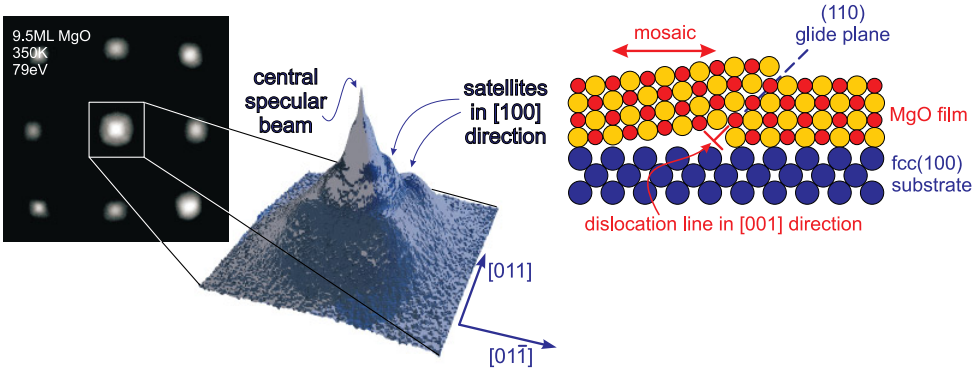

Figure 1. The LEED pattern of a MgO film 9.5 ML thick, prepared at 350 K by evaporation of Mg in an oxygen atmosphere of 3×10^{-5} Pa. The fourfold streaky broadenings in the high-symmetry directions due to the misfit dislocations are clearly visible. The corresponding model is shown in the right-hand part.

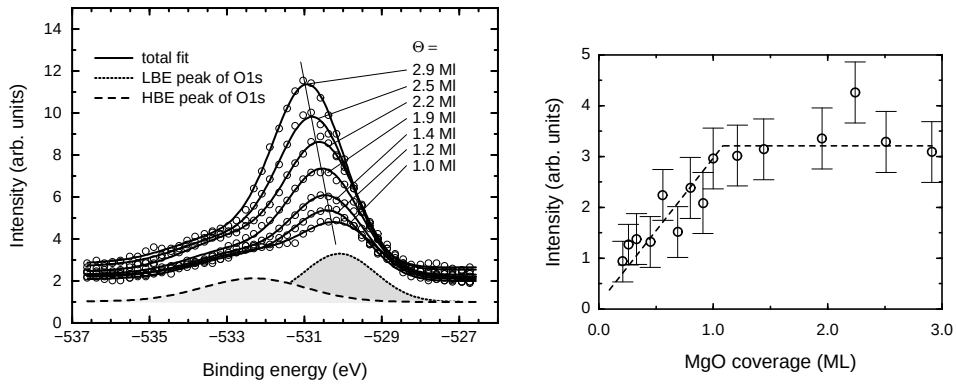

Figure 2. Left: O 1s spectra of oxidized Mg at $T = 300$ K in an oxygen atmosphere of 3×10^{-5} Pa for coverages Θ between 1 ML and 3 ML. The amounts deposited are indicated. Right: the dependence of the integral intensity of the HBE peak on the MgO coverage. The intensity of the MgO_2 species saturates exactly when the first monolayer is completed.

the HBE peak at 2.5 eV higher binding energy corresponds to a species chemically similar to MgO_2, as also concluded from systematic oxidation experiments, done with alkali halides, that also found an O 1s species at 2.5 eV higher binding energies next to the main peak identified with the formation of a peroxide species [20]. To determine the location of this species, we have measured the dependence of the integral intensity of the HBE peak on the MgO coverage, which was varied in small steps up to 2 ML. The result is shown in the right-hand part of figure 2. The integral intensity of the HBE peak saturates exactly as the first monolayer is completed. This provides clear evidence that the non-stoichiometric MgO_2 species is located on the surface within the first monolayer.

For all three different systems, we have carried out UPS and EELS investigations in order to identify defect-induced electronic states. However, none of the geometric imperfections discussed above—grain boundaries due to mosaic formation, dislocation networks, or elastic distortion—induced new electronic states that could be detected with our methods.

This negative finding might be partly due to the low concentration of defects, and partly also due to the too-small energy differences that should be expected in comparison with the ideal surface. The latter might be the case for the NaCl films, for which the maximum strain in the carpet across a Ge steps is 2% of the lattice constant. As will be seen below, however, this defect still has an effect on noble-gas adsorption that can be discriminated from that for the undisturbed parts of the films.

For the MgO films the concentration of surface atoms located at dislocations is estimated to be below 1%, which might be too low to be detectable. In the case of KCl(100) grown on NaCl(100), however, the concentration of defects due to the dislocation network, especially between 2 and 3 ML, should be high enough to be detectable, but again no signs of defect-induced electronic states have been found, as demonstrated by figure 3 for a KCl film 4 ML thick grown on 5 ML NaCl(100). On the contrary, from the EEL spectrum we obtained at the Γ point values for the band gap and the excitonic loss of 8.4 eV and 7.35 eV, respectively, which are in very good agreement with investigations of KCl(100) bulk crystals [2, 21].

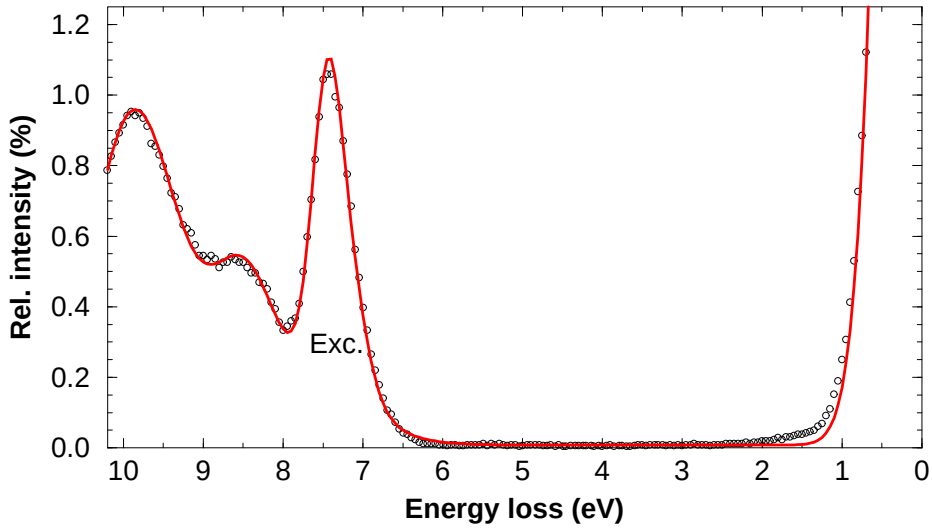

Figure 3. The EEL spectrum of epitaxially grown KCl(100) films. Primary electron energy: $E_0 = 40$ eV; specular direction: 60° off-normal. The solid line represents a fit done with Gaussian line shapes. $T = 300$ K.

3.2. Generation of anion vacancies

Point defects on alkali halides, which are spectroscopically active and visible in EELS as characteristic losses in the band gap, can be produced easily by electron bombardment. In figure 4 we show a high-resolution EEL spectrum of the NaCl(100) surface after bombardment with electrons at $T = 100$ K with an electron dose of 50 nA mm^{-2} for 30 minutes. The initially perfect band gap (similar to that of the KCl(100) EEL spectrum shown in figure 3) is modified by several losses located in the energy range between 1.0 and 2.7 eV, which can be assigned to losses of triplets (R_S at 1.2 eV), pairs (M_S at 1.5 eV), and single anion vacancies (F_S at 2.0 eV and at 2.7 eV) [22, 23] which act as colour centres. Qualitatively, the same behaviour was found for KCl(100) [22] in an experiment with lower resolution, but all peaks are shifted by about 25% to smaller loss energies.

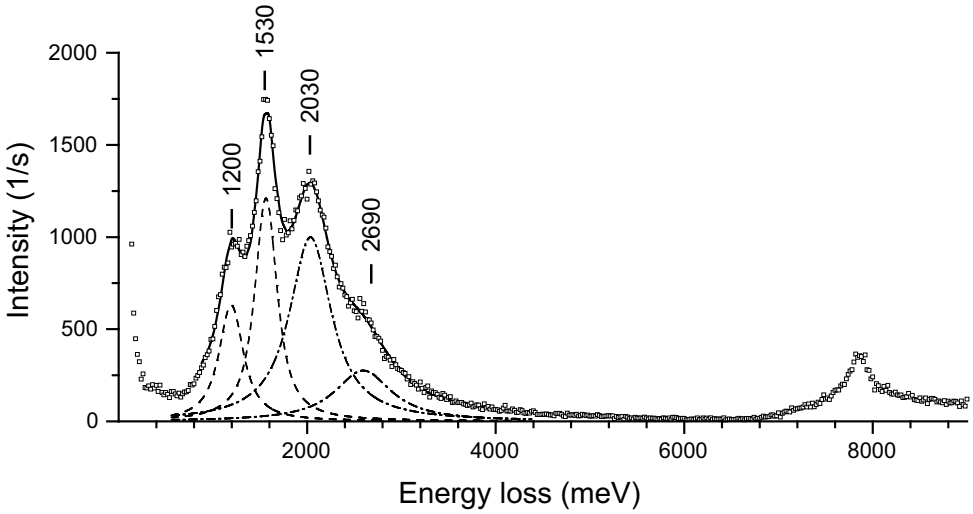

Figure 4. The EEL spectrum of colour centres of NaCl(100) after electron bombardment at temperatures below 100 K. For the assignment, see the text.

These colour centres are no longer stable at higher temperatures. Similar experiments carried out at room temperatures with lower resolution are shown in figure 5 (left-hand side). The NaCl(100) surface was bombarded with electrons with an impact energy of 195 eV and a current density of 140 nA mm^{-2}. Starting with a slightly damaged NaCl(100) surface (the lowest spectrum), EEL spectra were taken every two minutes. With progressing bombardment, the F_S peak at 2 eV saturates, while the loss peak at 3.4 eV grows with increasing electron exposure, and new peaks at 4.5 eV and 5.7 eV appear. Taking into account the results from Roy *et al* [24], we can say that the peaks labelled SP and BP in figure 5 correspond to electronic

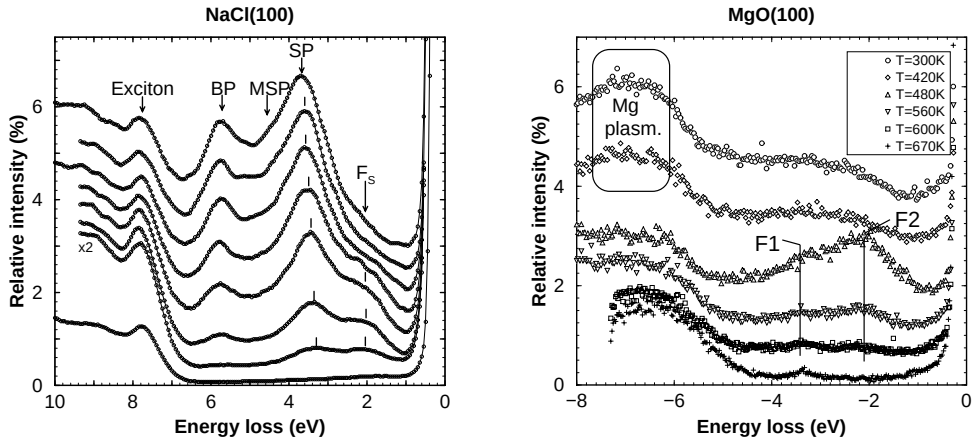

Figure 5. Left: EEL spectra of NaCl(100) at 300 K during electron bombardment ($E = 195$ eV; 140 nA mm^{-2}). BP, MSP, and SP denote excitations of bulk and surface plasmons from clusters of metallic Na. For improved clarity the spectra are shifted with respect to each other. Right: EEL spectra after the deposition of 5 ML of metallic Mg on top of 5 ML of MgO(100) and subsequent annealing up to the temperatures indicated.

losses of surface and bulk plasmons from Na clusters. Their energetic positions and the relative intensities change as functions of cluster size, but also as functions of the shape of the clusters. The observed shift of the surface plasmon-loss energy from 3.4 eV to 3.8 eV can be taken as an indication that the metallic Na particles transform from a pancake-like to a more spherical form. The shoulder which appears at 4.6 eV (denoted as MSP in figure 5) is most probably due to a high-order loss of the surface plasmon that should be energetically located at $0.8\overline{h}\omega_{BP}$ [25].

Similar spectra have been obtained after electron bombarding KCl(100) surfaces at lower substrate temperatures ($T = 260$ K) and lower current densities (40 nA mm^{-2}). The main difference in comparison with the NaCl(100) surface is that the energetic losses are typically 30% smaller and not as well resolved. The cross sections for production of colour centres are higher by at least a factor of five on KCl at the same electron energies.

In contrast, electron bombardment of MgO did not lead to detectable loss features in the band gap. However, an oxygen-depleted MgO surface can be produced by growth of MgO(100) films, as described above, and further evaporation of Mg at room temperature on top of the insulating surface followed by subsequent annealing to 480 K. A sequence of EEL spectra after growth and various steps of annealing is shown in figure 5. After deposition of 5 ML Mg on top of the MgO(100) film, the topmost EEL spectrum is obtained, with characteristic losses due to intra- and inter-band transitions of the metallic adlayer. The broad distribution of losses around 6–7 eV loss includes the loss of the Mg surface plasmon, which is expected at 7.35 eV [26], whereas the losses around 6 eV are more characteristic for surface plasmons of small spherical Mg particles. An increase of the substrate temperature up to 420 K leads to desorption of the multilayers of Mg [14]. After annealing to $T = 480$ K, two new peaks F1 and F2 with characteristic losses at 2.1 eV and 3.3 eV, respectively, are clearly visible in the band gap of MgO(100). These must be due to the presence of a more strongly bound submonolayer of Mg on the MgO surface. Due to these surplus Mg atoms, an oxygen-depleted MgO surface is generated, i.e. anion vacancies are formed right at the surface, as also confirmed by the absence of typical losses due to bulk F and F^+ centres [27] at around 5 eV. Also the edge due to the excitonic loss and the excitations from the valence to the conduction band has reappeared, demonstrating that the metallic layer has been removed. It should be pointed out that the resolution of the EELS instrument used in this experiment is much better than the halfwidths of the observed defect structure. Therefore, there seems to be a broad distribution of several configurations of defects, e.g. aggregates of colour centres, but also kinks and steps are possible. However, the method of production of these defects, the small shifts in spectroscopic features, and the good agreement with theoretical investigations [28] suggest that these F_S centres are neutral. Annealing to at least 670 K removes the surplus of Mg completely, and an EEL spectrum corresponding to a bare MgO(100) surface reappears. The small feature left at a loss energy of 3.4 eV is due to the plasmon loss associated with the MgO/Ag interface, as proven by a systematic variation of the film thickness of MgO. It disappears completely for thicker MgO layers or for smaller electron energies than that used here (50 eV).

3.3. Adsorption experiments: titration of defects

Defects increase the bonding strength strongly, and make the surfaces chemically reactive. This has been shown, e.g., by the dissociation of water at colour centres on both NaCl(100) and KCl(100) surfaces and by the stability of these OH^- centres up to 400 K [22, 29]. In contrast, molecular water adsorbs on defect-free alkali halides only at temperatures below 200 K [29–33].

Here we concentrate on another important piece of knowledge, that of the distribution and saturation concentration of point defects generated by electron bombardment with low-energy

electrons, as described above. The distribution of defects can be easily shown with LEED (see figure 6) to be random at temperatures where the chlorine vacancies produced by electron bombardment cannot migrate. This is the case at surface temperatures around 100 K. Figure 6 shows profiles of the (00) beam of a well ordered NaCl(100) film after various exposures to electrons ($E = 70$ eV, $j = 50$ nA mm^{-2}, $T = 100$ K). Although the intensity of the peak decreases rapidly with increasing exposure times, the width of the (00) beam remains unchanged. As expected, the background increases due to the creation of point defects induced by the electron bombardment. This indicates that the defects created by the electron beam are totally uncorrelated [34], i.e. they are distributed randomly on the surface.

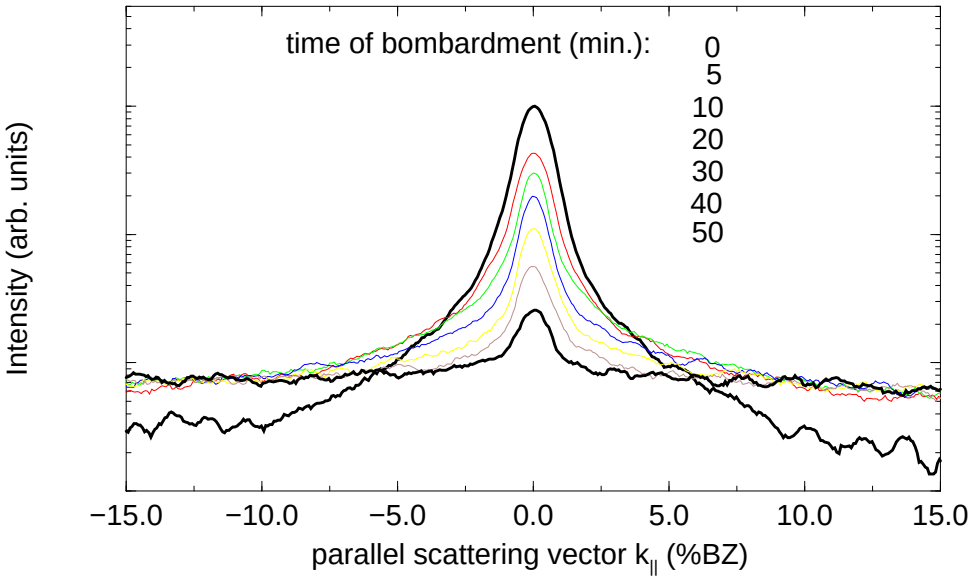

Figure 6. LEED 1D scans of the (00) spot after various exposures to electrons (electron energy 70 eV, current density 50 nA mm^{-2}) at a surface temperature of 100 K. The spectra are not shifted. The bold lines mark profiles before and after the completed exposure to electrons (small peak).

The saturation concentration of surface colour centres produced by electron bombardment was determined by titration experiments with noble gases and with CO_2 using thermal desorption spectroscopy. This information is obtained from the changes in kinetics and energetics of the noble-gas layers induced by point defects, and from the fact that the saturation concentration can be easily determined for these gases by combining LEED and TDS. Different inert gases yield similar results in terms of the saturation concentration of defects. They differ, however, in the details of the kinetics and energetics observed [35]. Here we concentrate on experiments with Kr.

TPD data for Kr from the undistorted substrate are shown in the left-hand part of figure 7. Evolution of a second desorption peak is coupled with the completion of the monolayer, which grows isomorphically with the substrate, as found with LEED. Therefore, the first Kr layer has the same density as the substrate surface. The common leading edge of all spectra from submonolayer coverages indicates zeroth-order desorption. This property is characteristic for desorption very close to thermodynamical equilibrium between a 2D solid and a 2D gas of low concentration and high mobility.

In the presence of point defects, this behaviour changes completely, as seen on the right-

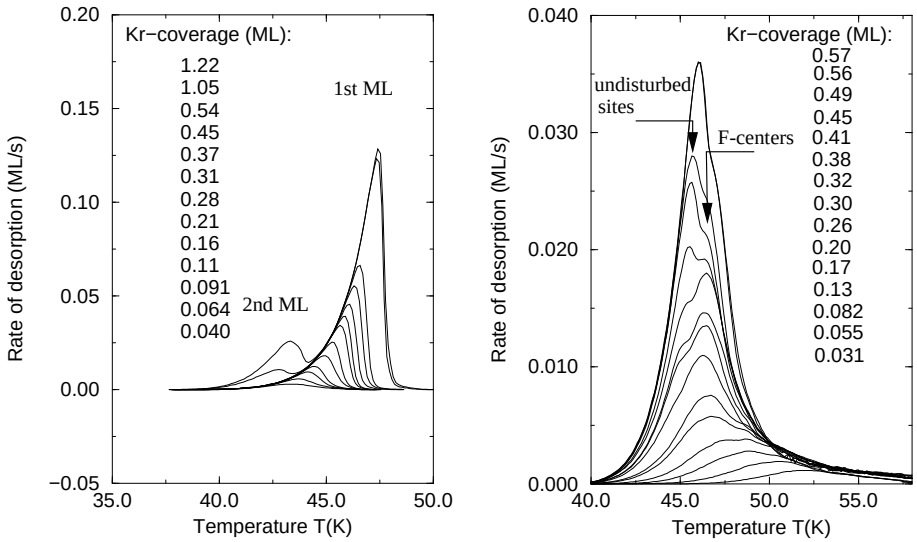

Figure 7. TD spectra of Kr on undamaged NaCl(100) (left) and on NaCl(100) with a saturation concentration of colour centres (right).

hand side of figure 7. These TD curves have been obtained after saturation of the defect concentration was reached, as concluded from the constant shape of the TPD spectra, at 0.5 ML coverage of Kr after a further increase of the electron dose. Two main effects can be seen. First, the centre of the spectra at constant coverage is shifted to higher temperatures by about 2 K, indicating an enhanced binding strength at the defect sites. Second, the previous monolayer desorption peak is split into two states. This is coupled with a transition from zero- to first-order desorption, as found by a detailed analysis of the curves [35], indicating the destruction of the equilibrium between 2D gas and 2D solid. This is due to energetic inhomogeneities on the surface caused by the vacancies, for which the adsorbed Kr atoms are used as sensors.

In order to obtain quantitative information about the influence of the vacancies on the adsorbed Kr atoms, a large set of data for up to half a monolayer have been evaluated for the undamaged surface and for a saturation concentration of colour centres. Both leading-edge and full isosteric analyses have been used. The results from the two methods agree within the limits of uncertainty indicated by the scatter of the data. They are shown in figure 8.

For the undamaged surface an effective binding energy of 13 kJ mol^{-1} is found independently of the Kr concentration. This is compatible with the above-mentioned equilibrium between 2D gas and 2D solid. It means that desorption takes place exactly along the line of coexistence. As a consequence, the rates of desorption only depend on temperature, and not on coverage, down to a remaining coverage of approximately 3% of a monolayer. Only in this very-low-coverage regime was an increase of the pre-exponential factor by roughly one order of magnitude found, coupled with a change to first-order desorption, and a slight increase in binding energies. This finding indicates also that the undamaged surface is not completely free of sites with higher binding energy than the perfect NaCl surface. This property is not unexpected for our films elastically strained across steps of the Ge substrate. Although the average terrace length of the Ge surfaces used is around 100 lattice constants [7], the distribution

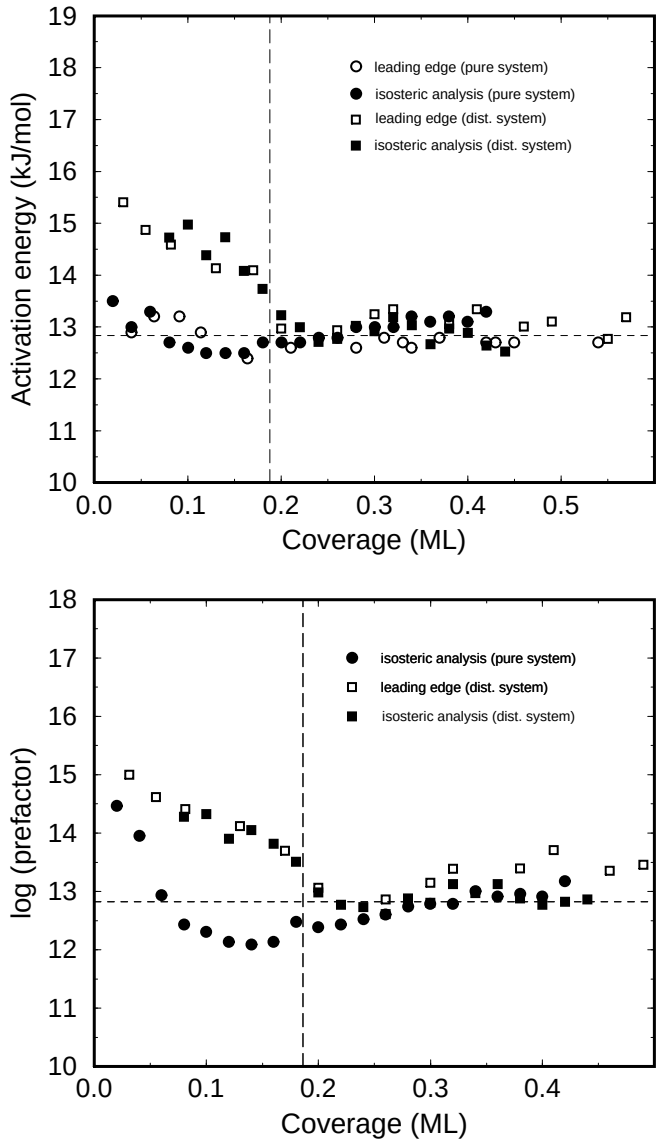

Figure 8. Isosteric heats of desorption and pre-exponential factors of Kr from undamaged NaCl(100) surfaces and from surfaces with a saturation concentration of colour centres. The isosteres have been determined from TDS spectra like those shown in figure 7 by back-integration.

of the strain over many lattice constants in the NaCl film makes the relatively large fraction of adsorbed Kr atoms bound more strongly than on the flat terraces understandable. In addition, there might also be a small concentration of steps and dislocations present on the surface. The stronger bonds tend to localize the Kr atoms, leading to the observed increase of the pre-exponential factor at these low coverages. These additional defects, which are all neutral, cause relatively small changes of local environments, compared with those at a vacancy. Therefore, only small peak shifts of a few tenths of an eV at most are expected in both types of electron

spectroscopy used here. This makes them hard to detect by UPS of EELS, especially at the low concentrations present on the undamaged surface. Indeed, they have only been detected indirectly from, e.g., the small water-induced features in UPS still present close to 180 K. Water on the perfect surface desorbs at around 150 K. Thus it turns out that titration experiments are in practice more sensitive to these types of defect than electron spectroscopy.

On the surface saturated with colour centres, the increase of both the binding energy and the pre-exponential factor is much more drastic. For coverages lower than 0.18 ML the binding energy increases from 13 kJ mol^{-1} by almost 25% to 16 kJ mol^{-1} close to zero coverage. In the same coverage range, the pre-exponential factor increases by two orders of magnitude for low coverages—from 10^{13} to 10^{15} s^{-1}. The much larger increase of binding energies at low coverages on the defect-rich surface indicates that the defects on the undamaged surface, which exist in small concentrations, are not identical to the colour centres produced by electron bombardment. The former species might consist mainly of steps, kinks, and dislocations, whereas the latter are mainly chlorine vacancies. The gradual decreases of binding energies as well as of the values of the pre-exponential factors as functions of coverage indicate that a mixture of different geometric configurations of defects is present on the surface, consistent with the finding with EELS (see figure 4). In particular, M and R centres are most probably filled with more than one Kr atom. It is conceivable that the binding energy of such groups depends on the number of noble-gas atoms located on the defect. This would explain the gradual change of both the isosteric heats of adsorption and of the pre-exponential factors. At the lowest coverages, only the sites with the strongest bonds and the highest localization remain occupied.

This leads to the question of the actual concentration of defects. It is obvious that the density of Kr atoms cannot be increased beyond the concentration on the undamaged surface, even at defect sites, since bonding still occurs by means of van der Waals forces also at the defect sites, so an effective change of the atomic radii of Kr atoms is implausible. On the other hand, the fast decrease of the van der Waals interaction will limit the influence of the defects mostly to the noble-gas atoms located exactly on the defect sites. Therefore, we expect the number of Kr atoms bound more strongly than on the undamaged surface to be roughly equal to the number of atomic vacancy sites created. This number would only change if large geometric relaxations happened in the vicinity of such vacancies, which is not very likely. Therefore, our titration experiment allows an estimate of the saturation density of surface colour centres of between 15–20% of a monolayer to be obtained.

In conclusion, we have demonstrated for the examples of NaCl, KCl, and MgO epitaxial thin films that such films can be produced with relatively good crystalline quality. They contain, however, defect sites in the form of steps, kinks, and dislocations whose concentration is characteristic for the combination of materials. This sort of defect does not produce new electronic states, but may modify the binding strength of atoms and molecules due to enhanced dipolar interaction. Atomic vacancies like the colour centres investigated here in more detail can have a much larger effect, as already seen from the adsorption of noble gases. Our experiments show that they can be produced in high concentration on alkali halide surfaces. As demonstrated by other experiments performed by our group [22], they are also chemically highly reactive.

Acknowledgments

The support given by the Deutsche Forschungsgemeinschaft through the Forschergruppe ‘Adsorbatwechselwirkungen an Ionenkristallen und Metallen’ and the Kali und Salz GmbH is gratefully acknowledged.

References

[1] Creuzburg M 1966 *Z. Phys.* **196** 433
[2] Roessler D and Walker W 1968 *Phys. Rev.* **166** 599
[3] Henrich V E and Cox P A 1994 *The Surface Science of Metal Oxides* (Cambridge: Cambridge University Press)
[4] Bandet-Faure J and Touzilier L 1974 *Surf. Sci.* **43** 183
[5] Pian T, Tilk N, Traum M, Kraus J and Collins W 1983 *Surf. Sci.* **129** 573
[6] Ammer C, Meinel K and Klaua M 1995 *Phys. Status Solidi* a **150** 507
[7] Schwennicke C, Schimmelpfennig J and Pfnür H 1993 *Surf. Sci.* **293** 57
[8] Hebenstreit W, Redinger J, Horozova Z, Schmid M, Podloucky R and Varga P 1999 *Surf. Sci.* **424** L229
[9] Fölsch S, Meyer G and Rieder K H 1998 private communication
[10] Henzler M, Homann C, Malaske U and Wollschläger J 1995 *Phys. Rev.* B **52** R17 060
[11] Henzler M 1993 *Prog. Surf. Sci.* **42** 297
[12] Wollschläger J, Viernow J, Tegenkamp C, Erdös D, Schröder K M and Pfnür H 1999 *Appl. Surf. Sci.* **142** 129
[13] Wollschläger J, Schäfer F, Erdös D, Schröder K M, Michailov M and Henzler M 1997 *Surface Diffusion: Atomistic and Collective Processes (NATO ASI series B, vol 360)* (New York: Plenum) p 235
[14] Tegenkamp C, Michailov M, Wollschläger J and Pfnür H 1999 *Appl. Surf. Sci.* **151** 40
[15] Wollschläger J, Erdös D and Schröder K M 1998 *Surf. Sci.* **402–404** 272
[16] Peterka D, Tegenkamp C, Schröder K M, Ernst W and Pfnür H 1999 *Surf. Sci.* **431** 146
[17] Corneille J S, He J W and Goodman D W 1993 *Surf. Sci.* **306** 269
[18] Burke M L and Goodman D W 1994 *Surf. Sci.* **311** 17
[19] Ochs D, Maus-Friedrich W, Brause M, Günster J, Kempter V, Puchin V, Shluger A and Kantorovich L 1996 *Surf. Sci.* **365** 557
[20] Jupille J, Dolle P and Beancon C R 1992 *Surf. Sci.* **260** 271
[21] Tomiki T 1969 *J. Phys. Soc. Japan* **26** 738
[22] Malaske U, Tegenkamp C, Henzler M and Pfnür H 1998 *Surf. Sci.* **408** 237
[23] Henzler M, Thielking D, Horn-von Hoegen M and Zielasek V 1998 *Physica* A **261** 1
[24] Roy G, Singh G and Gallon T 1985 *Surf. Sci.* **152+153** 1042
[25] Inglesfield J and Wikborg E 1975 *J. Phys. F: Met. Phys.* **5** 1706
[26] Rocca M 1995 *Surf. Sci. Rep.* **22** 40
[27] Chen Y, Williams R T and Sibley W A 1969 *Phys. Rev.* **182** 960
[28] Paccioni G, Ferrari A M and Ierano G 1996 *Faraday Discuss.* **255** 58
[29] Fölsch S and Henzler M 1991 *Surf. Sci.* **247** 269
[30] Fölsch S, Barjenbruch U and Henzler M 1989 *Thin Solid Films* **127** 123
[31] Barraclough P and Hall P 1989 *Surf. Sci.* **211+212** 749
[32] Heidberg J and Häser W 1991 *J. Electron Spectrosc. Relat. Phenom.* **54/55** 971
[33] Kantorovich L and Shlyuger A 1984 *Sov. J. Chem. Phys.* **1** 2277
[34] Henzler M 1977 Electron diffraction and surface defect structure *Electron Spectroscopy for Surface Analysis* ed H Ibach (Berlin: Springer) p 117
[35] Ernst W, Kramer J and Pfnür H 1999 in preparation